DOI: 10.1021/ma900227t

Macromolecules
ARTICLE

Hydrogen-Bonded Polymer Nanotubes in Water

Anja Gress,[†,∥] Anne Heilig,[†] Bernd M. Smarsly,[‡] Matthias Heydenreich,[§] and Helmut Schlaad*[,†]

[†]*Max Planck Institute of Colloids and Interfaces, Research Campus Golm, 14424 Potsdam, Germany,* [‡]*Justus Liebig University Giessen, Institute of Physical Chemistry, Heinrich-Buff-Ring 58, 35392 Giessen, Germany, and* [§]*University of Potsdam, Institute of Analytical Chemistry, Karl-Liebknecht Str. 24-25, 14476 Golm, Germany.* [∥] *Present address: BASF SE, Ludwigshafen, Germany.*

Received February 2, 2009; Revised Manuscript Received March 23, 2009

ABSTRACT: Intermolecular hydrogen bonding, not hydrophobic interaction, is the driving force for the spontaneous self-assembly of glycosylated polyoxazoline chains into nanotubes in dilute aqueous solution. The structural information is encoded in the relatively simple molecular structure of chains consisting of a tertiary polyamide backbone (hydrogen-accepting) and glucose side chains (hydrogen-donating). The formation of the nanotubes should occur through bending and closing of a 2D hydrogen-bonded layer of interdigitated polymer chains.

Introduction

Block copolymer colloids have great potential in the fields of composite materials[1] and biomedical applications[2] and also for the bioinspired generation of hierarchical structures.[3]

Conventionally, the self-assembly of block copolymers in an aqueous environment is driven by the hydrophobic effect, which involves the dehydration and subsequent aggregation of the hydrophobic chains to minimize contact with water. In terms of thermodynamics, the aggregation of amphiphiles occurs because of entropic contributions to the free energy. The shape of the resulting structure (spherical or cylindrical micelle or vesicle) depends on the value of the geometric packing parameter of the amphiphile.[4−7]

Despite their omnipresence in biological systems[8] and in supramolecular chemistry,[9,10] enthalpic hydrogen bonding interactions have scarcely been employed for the self-assembly of polymers into discrete structures in aqueous (!) solutions. Examples reported so far involve block copolymers that comprise β-sheet-forming peptide sequences or designed cyclic peptides forming fibrillar superstructures or nanotubes in aqueous solution.[3,11,12] In these cases, the motif of the intermolecular hydrogen bonding interactions and the resulting superstructure is covalently encoded in the particular peptide sequence.

As proposed earlier by us,[13] a sequence of amino acids (or nucleotides, etc.) may not be needed to induce a self-assembly of polymer chains via intermolecular hydrogen bonding. The code could be as simple as a synthetic homopolymer, for instance, a glycosylated polyoxazoline, poly[2-(4-(β-D-glucosylsulfanyl)-butyl)-2-oxazoline] (Figure 1a, R = H), having hydrogen-accepting tertiary amide units in the backbone (hydrophilic)[14] and hydrogen-donating hydroxyl groups in the side chains (hydrophilic). These polymers are, unlike other glycopolymer homopolymers (e.g., poly[2-(β-D-glucosyloxy)ethyl acrylate]),[15] considered to be nonamphiphilic in nature. Three polymer samples (including the sample from ref 13) with different molecular weights were found to assemble spontaneously into hydrogen-bonded nanotubes in water as well as in dimethylsulfoxide, as evidenced by scanning force microscopy (SFM), small-angle X-ray scattering (SAXS), and spectroscopy (FT-IR and 2D-NOESY NMR). Here we present a refined picture of the mechanism of formation and the structure of these polymer nanotubes.

Experimental Part

Polymer Synthesis. Three glycosylated polyoxazoline samples were prepared by ring-opening isomerization polymerization of 2-(3-butenyl)-2-oxazoline and subsequent quantitative photoaddition of 2,3,4,6-tetra-*O*-acetyl-1-thio-β-D-glucopyranose onto the vinyl double bonds, as described earlier.[16] The glycopolymers (chemical structures in Figure 1a) exhibited number-average degrees of polymerization of n = 21 (**1a**), 63 (**2a**), and 126 (**3a**) (^{1}H NMR) and polydispersity indexes of PDI $\approx$ 1.1 (size exclusion chromatography, SEC). The acetyl protecting groups were removed by treatment with sodium methoxide in chloroform solution at room temperature (→ **1b**, **2b**, and **3b**).[13] The quantitative deacetylation of the glucose units was confirmed by Fourier transform infrared (FT-IR) spectroscopy. (See Figure 1b.) Products were purified by dialyses against deionized water and isolated by freeze drying. ^{1}H NMR (400 MHz, D_2O, δ): 1.67 (bs, 4H), 2.32−2.43 (m, 4H), 2.77−2.84 (bs, 2H), 3.32−3.36 (t, 1H), 3.53−3.61 (m, 12H), 3.70−3.74 (m, 1H), 3.90−3.93 (d, 1H), 4.54−4.56 (d, 1H). FT-IR ($\tilde{\nu}$/cm^{-1}): 3300 (O−H), 2920 (C−H str), 1613 (NC═O str, amide I), 1420 (CH_2−CO).

^{1}H NMR measurements were carried out at room temperature using a Bruker DPX-400 spectrometer operating at 400.1 MHz. D_2O was used as solvent (Deutero GmbH, Germany), and signals were referenced to the signal of solvent at δ 4.79. 2D-^{1}H,^{1}H-NOESY-NMR spectra were recorded in dimethylsulfoxide (DMSO-d_6) at room temperature with a Bruker Avance 500 spectrometer operating at 500.17 MHz. Spectra were measured with 48 scans and mixing times of 150 or 600 ms. The Bruker standard software package was used for acquisition (XWIN-NMR 3.5) and processing (TopSpin 1.3) of data. FT-IR spectra were recorded on a BioRad 6000 FT-IR; samples were measured in the solid state using a single reflection diamond ATR. SFM measurements were performed on a Nanoscope Multimode IIIa microscope (Digital Instruments, Santa Barbara, CA) using silicon cantilevers having k = 42 N/m (Nanoworld, Switzerland). The surface was scanned at room temperature in tapping mode at a resonance frequency of 200−300 kHz. Samples were prepared by spin-coating 0.01 to

*Corresponding author. Fax: +49.331.567.9502. E-mail: schlaad@mpikg.mpg.de.

 Published on Web 05/08/2009

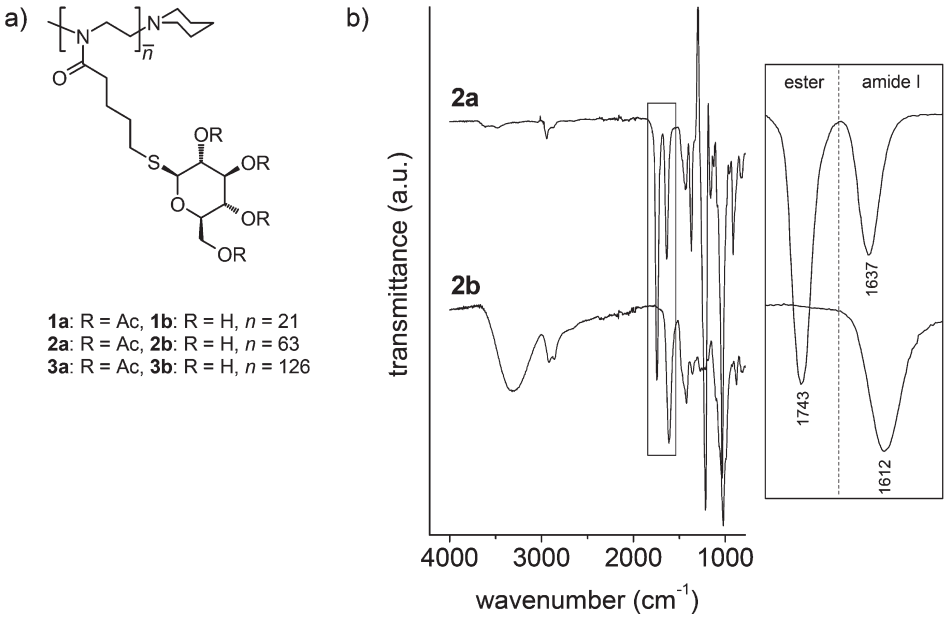

Figure 1. (a) Chemical structure of the glycopolymers **1**−**3** (**a**: acetyl protected form, **b**: deprotected form) and (b) exemplary FT-IR spectra (including an enlargement of the region of the carbonyl bands) of **2a** and **2b**.

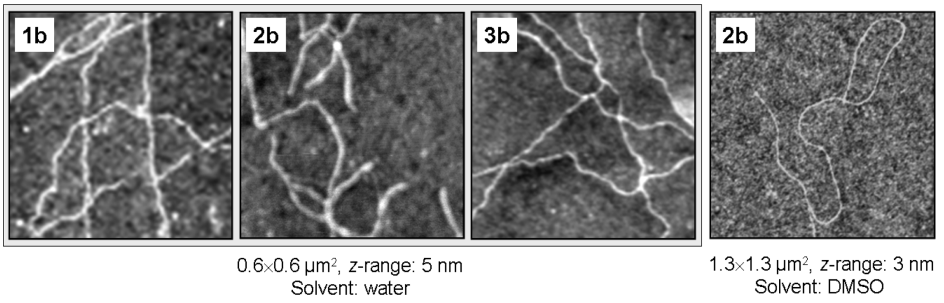

Figure 2. SFM height images of specimens obtained by spin-coating of dilute aqueous solutions of **1b** (0.01 wt %), **2b** (0.05 wt %),[13] and **3b** (0.01 wt %) and DMSO solution of **2b** (0.03 wt %) on silicon substrates.

0.05 wt % polymer solutions at 3000 rpm onto a silicon waver. SAXS was done at room temperature using a Bruker AXS "Nanostar" setup with a Cu Kα radiation source and pinhole collimation. The distance between the capillary containing a 10 wt % aqueous polymer solution and the 2D detector was 105 cm. The 2D patterns were transformed into a 1D radial average of the scattering intensity.

Results and Discussion

Aqueous solutions of the glycopolymers **1b**, **2b**, and **3b** (degree of polymerization, n = 21, 63, and 126, respectively) were first investigated by SFM and by SAXS. The SFM imaging of samples prepared by spin-coating of dilute solutions containing 0.01 to 0.05 wt % polymer revealed the presence of fibers that were hundreds of nanometers in length. (See Figure 2.) Cross-sectional analyses yielded average widths of the fibers of $b \approx 15$ (**1b**), 20 (**2b**), and 16 nm (**3b**) at heights of $h < 1$ nm (Table 1). The low values for the height seem to indicate, at a first glance, that fibers could have a tapelike structure in which polymer backbones would be oriented perpendicular to the fiber long axis. However, there is no direct correlation between the width of the fibers and the contour length (l_c) of the fully stretched backbones in all-trans conformation. A tapelike structure can be excluded, especially for **1b** because the width of the fiber by far exceeds the dimension of the chain (not for **2b** and **3b**). An alternate structure for all three samples is that of a hollow nanofiber or nanotube in which polymer chains are oriented parallel to the long axis.[13] Interactions with the silicon substrate lead to a collapse of the fibers. Depending on whether the measured height corresponds to one or two layers of polymer, the width would be a measure of the circumference or the diameter of the tubular cross-section, respectively. The original diameters of the tubes in solution would then have been on the order of 4 to 10 nm. (See below.)

Table 1. Contour Lengths ($l_c = 0.36 \cdot n$ nm) of Glycopolymers 1b, 2b, and 3c and Average Widths (b) and Heights (h) of Corresponding Collapsed Fibers on Silicon Substrates (SFM)[a]

sample	l_c (nm)[a]	b (nm)[b]	h (nm)[b]	water/DMSO[c]
1b	8	14.7 ± 3.3	0.8 ± 0.1	●/−
2b	23	20.2 ± 1.9	0.7 ± 0.2	●/−
		27.1 ± 1.4	0.7 ± 0.2	−/●
3b	45	16.7 ± 5.2	0.7 ± 0.2	●/−

[a] Assuming an all-trans conformation of the backbone (segment length of a repeat unit, −N−C−C− = 3.6 Å; number of monomer units = n). [b] Average values from 20 single measurements. [c] Solvent used.

For more detailed information on the original morphology and dimension of nanofibers, aqueous solutions of **1b**, **2b**, and **3b** (10 wt %) were analyzed by SAXS. It should be noted that for the sake of reasonable data quality SAXS measurements had to be performed at much higher concentrations than the SFM investigations. All three scattering curves (Figure 3) indicate that the asymptote of the SAXS curve at large scattering vectors $q = (4\pi/\lambda) \cdot \sin\theta$ (λ: wavelength of X-ray beam, θ: scattering angle) approximately obeys the characteristic dependence $I(q) \propto q^{-1}$ (I: intensity) for thin elongated objects, that is, nanofibers. For **2b**

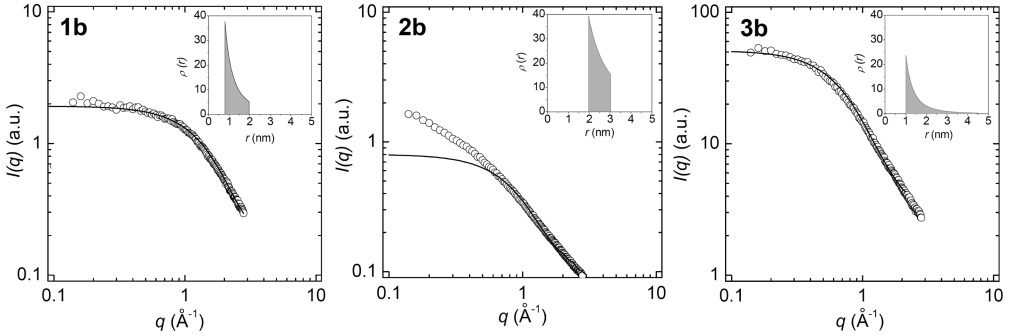

Figure 3. SAXS data obtained for 10 wt % solutions of **1b**, **2b**,[13] and **3b** in water. The solid lines represent the fits of the data to the form factor of a hollow cylinder of infinite length; insets show the radial density profiles of the fitted scattering curves.

only, however, a continuous increase in the scattering intensity toward small q was recognized, which might be attributed to the coexistence of larger objects (vesicles).[13] Unfortunately, the curves do not show form factor oscillations, which would allow an unambiguous analysis in terms of the shape and dimension of aggregates. Hence, we analyzed data by different models, thereby trying to determine the most probable structure. In particular, these models were hollow tubes and compact cylinders with a circular cross-section and infinite length; the general approach developed by Burger and Förster was used for the corresponding model functions.[17] This approach enables one to analyze scattering data of polydisperse objects and core−shell structures. Also, a nonconstant radial profile of scattering length density can be considered using algebraic density profiles $\phi(r) \approx r^{\alpha}$. In this approach, the density profile consists of piecewise analytical functions $\phi(r)$ in each of a number of concentric microdomains of a compartmented particle, here a tube.

The structural fitting parameters were the outer and inner radius (r_o and r_i), the latter being zero for compact cylinders, the polydispersity of the outer radius and a radial density profile (r^{α}), and a constant background scattering, I_B. More fitting parameters were not used in light of the featureless curves. The best possible fits of the SAXS data (solid lines in Figure 3) were obtained with the model of hollow tubes; good fits to a compact cylinder were only obtained when the polydispersity of the radius took unrealistic values. The values obtained for r_o and r_i of the tubes are summarized in Table 2: r_o/r_i = 2.0/0.8 (**1b**), 3.0/2.0 (**2b**), and 4.5/1.0 nm (**3b**). The radial density profiles of the fitted scattering curves show all of the characteristic behaviors of hollow structures because the electron density decreases from the inner to the outer part. (See the insets in Figure 3.) The profiles of **1b** and **2b** indicate a rather sharp interface between the wall and the solvent phase; the walls have a thickness of $(r_o - r_i) \approx 1$ nm. In the case of **3b**, the interface is apparently thicker (3.5 nm) but also more diffuse; the highest density is at r = 1 to 2 nm. It could be assumed that, for entropic reasons, not all polymer segments are integrated in the cylinder wall but are extended from the wall like hairy layers. (See the structure illustration in Table 2.)

SFM and SAXS results seem to support the existence of nanotubes rather than that of tapes; nevertheless, some uncertainty persists. Attempts to visualize the fibers in a noncollapsed state and to have a look at the inner structure, for instance by cryogenic transmission microscopy, were not successful so far, which might be attributed to glucose−water interactions causing problems with the cryofixation of aggregates.[18] It should further be mentioned that tubular vesicles with a bilayered membrane can be excluded because of the large curvature of the structure.[13]

As previously discussed,[13] the wall should be constructed of polymer chains forming a sheet through intermolecular hydrogen bonding interactions between the tertiary amides of the backbone (H-accepting) and pendant glucose units (H-donating). In FT-IR

Table 2. Outer and Inner Radii (r_o and r_i) and Wall Thicknesses ($r_o - r_i$) of the Hollow Nanofibers of Glycopolymers 1b, 2b, and 3b in Water (SAXS)

sample	r_o (nm)	r_i (nm)	$r_o - r_i$ (nm)	structure
1b	2.0 ± 0.3	0.8 ± 0.1	1.2 ± 0.4	
2b	3.0 ± 0.4	2.0 ± 0.5	1.0 ± 0.9	
3b	4.5 ± 0.5	1.0 ± 0.2	3.5 ± 0.7	

(Figure 1b), the amide I vibration of **2b** arises at a lower wavenumber (1612 cm^{-1}) or frequency than that of **2a** (1636 cm^{-1}), which is attributed to the existence of NC═O···HO hydrogen bonds.[19]

We applied 2D-^{1}H,^{1}H-NOESY NMR spectroscopy[20] to have a closer look at the possible structure of the polymer layer. The nuclear Overhauser effect (NOE) allows for the detection of interactions between atoms in space within a distance of less than 5 Å. For polymers, usually negative NOEs are measured, and mixing times are chosen according to the relaxation times of side chains (600 ms) and backbones (150 ms). To be able to detect the signals of the hydroxyl protons of the glucose units, however, measurements had to be performed in DMSO-d_6 as the solvent instead of D_2O. The existence of nanofibers in DMSO solution was exemplarily confirmed for **2b** by SFM (Figure 2). The 2D-NMR spectrum of **2b** in DMSO-d_6 (mixing time: 600 ms) is shown in Figure 4. It indicates, among others, strong correlations between the protons of the hydroxyl groups of the glucose unit (13, 14, 15, and 16, δ 4.5 to 5.1) and the protons of two methylene groups of the side chain (4 and 5, δ 1.5 to 1.6). NOEs between the glucose protons and the methylene groups 3 and 6 (side chain) and 1 and 2 (backbone) could not be detected. However, at a mixing time of 150 ms, all signals appear to be much broader, and NOEs between the hydroxyl and methylene protons vanished (data not shown). This observation could be attributed to a highly dynamic nature of the structure.

With all of this information, one can draw a tentative structure model of the polymer layer, as illustrated in Figure 5. Ideally, the polymer backbone adopts an all-trans conformation, and neighboring glucose side chains point in opposite directions (optimized geometry). The 2D growth of the layer occurs via intermolecular hydrogen bonding between tertiary amide and glucose units. The polymer layer bends and closes to a tube during the growth process. A similar mechanism has previously been described for the formation of amphiphilic polymer vesicles.[7] Bending and closure is driven by line tension, which arises from the exposure of the hydrophobic chains to water at the rim of the sheet or layer. The size of the vesicle is then determined by the flexibility or bending modulus of the sheet. Here line tension could result from unsaturated hydrogen bonds at the rim of the layer. The reason why the layer closes to a tube and not to a sphere could be different flexibilities along and perpendicular to the polymer

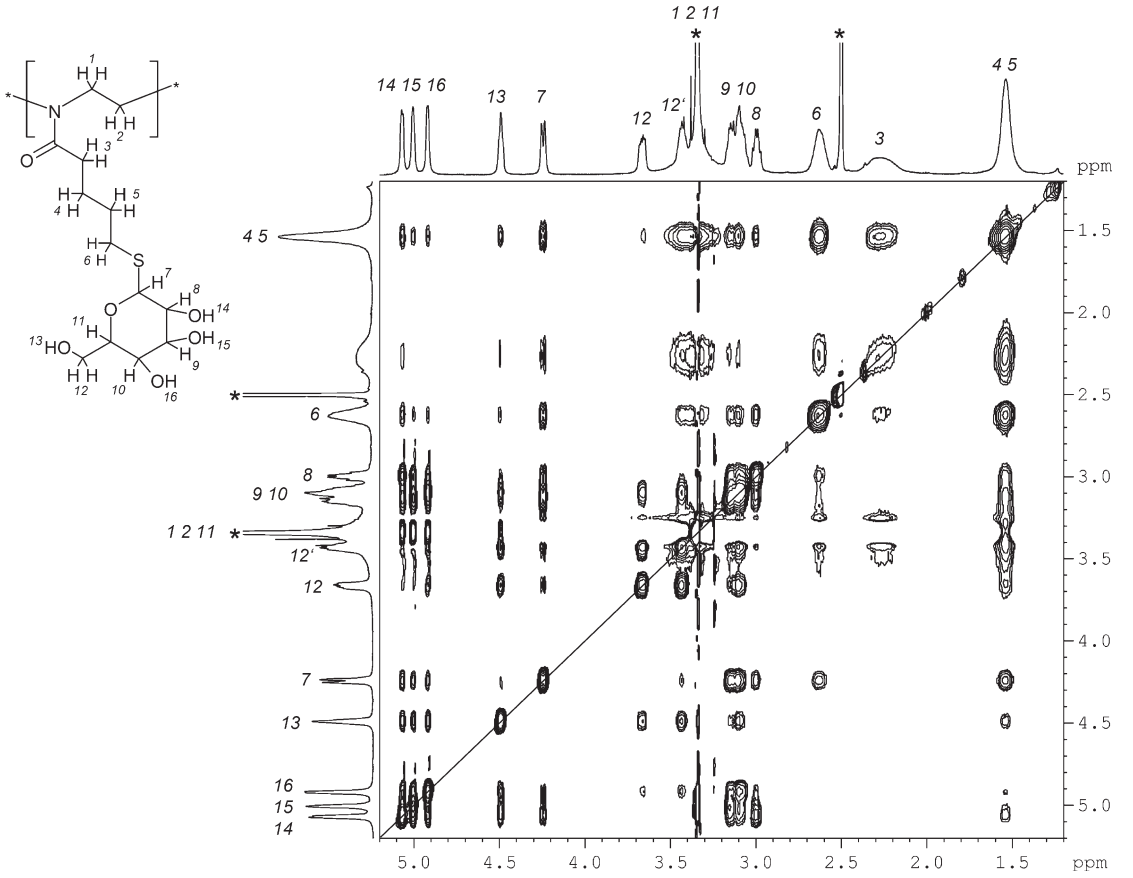

Figure 4. 2D-^{1}H,^{1}H- NOESY NMR spectrum (500.17 MHz, mixing time: 600 ms, negative levels) of a 2 wt % solution of **2b** in DMSO-d_6 (* = solvent).

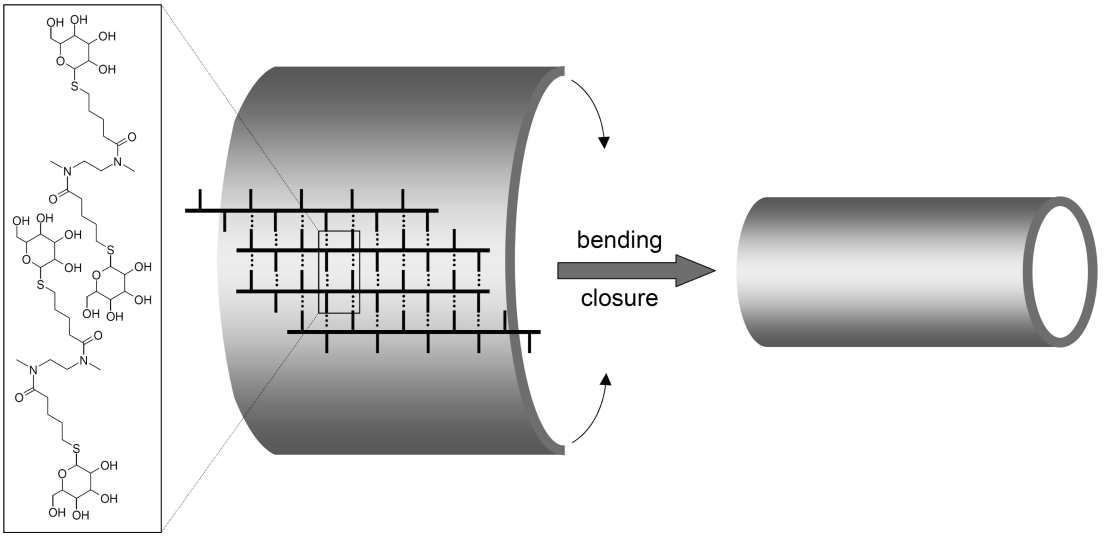

Figure 5. Tentative idealized structure of the hydrogen-bonded glycosylated polyoxazoline layer (hydrogen bonds are indicated as dotted lines) and subsequent bending and closing into a nanotube.

chain. Evidently, the layer should be more flexible in the direction of the hydrogen bonds than in the direction of the covalent bonds of the backbone. The diameter of the tube should be dependent on the nature of the solvent, especially on its hydrogen-bonding ability. In fact, tubes are significantly smaller in water than they are in the moderately hydrogen-bonding aprotic solvent DMSO (Table 1).[21]

However, the glycopolymer nanotubes are built upon hydrogen bonds and should therefore be treated as a dynamic structure. Owing to the competitive hydrogen bonding of the solvating water molecules, not all glucose units may be involved in hydrogen bonding with the polymer backbone at the same time and eventually point out of the layer plane into the aqueous phase and thus contribute to the stabilization of the nanotubes in solution. Glucose units may also be reversibly coordinated to the same polymer chain (intra- versus intermolecular hydrogen bonding). It is further noteworthy that the formation of the nanotubes is an open aggregation process, which is subject to change with concentration and time. However, changes in concentration may affect the length of the nanotubes but not the thickness of their wall (as evidenced by the comparison of SFM and SAXS data at different concentrations).

Conclusion

Intermolecular hydrogen bonding (NC═O···HO) between glycosylated polyoxazoline chains (FT-IR) leads to the spontaneous formation of nanotubes, measuring a few nanometers in diameter and hundreds of nanometers in length (SFM and SAXS), in aqueous solution. It is supposed that the initially formed 2D layer of interdigitated polymer chains (NMR) bends and closes to a tube, driven by line tension, by analogy to the elaborated mechanism for the formation of polymer vesicles.

Future work is devoted to the refinement of the mechanism and extension of the concept of hydrogen-bonded structure formation in aqueous solution. Following the examples in biological systems (e.g., the folding of proteins or the production of collagen fibers), it is thought to implement additional noncovalent interactions, especially hydrophobic and electrostatic interactions, to obtain more complex and hierarchical structures.

Acknowledgment. Ines Below, Jessica Brandt, Olaf Niemeyer, Ingrid Zenke, Antje Völkel, Helmut Cölfen, Markus Antonietti, and Erich C. are thanked for their contributions to this project. Financial support was given by the Max Planck Society and, as a part of the EUROCORES Programme BIOSONS, by the German Research Foundation.

References and Notes

(1) Balazs, A. C.; Emrick, T.; Russell, T. P. *Science* **2006**, *314*, 1107–1110.
(2) Duncan, R. *Nat. Rev. Drug Discovery* **2003**, *2*, 347–360.
(3) Börner, H. G.; Schlaad, H. *Soft Matter* **2007**, *3*, 394–408.
(4) Evans, D. F.; Wennerström, H. *The Colloidal Domain: Where Physics, Chemistry, Biology, and Technology Meet*; VCH: New York, 1994.
(5) Jain, S.; Bates, F. S. *Science* **2003**, *300*, 460–464.
(6) Discher, D. E.; Eisenberg, A. *Science* **2002**, *297*, 967–973.
(7) Antonietti, M.; Förster, S. *Adv. Mater.* **2003**, *15*, 1323–1333.
(8) Stryer, L. *Biochemistry*; W. H. Freeman & Company: New York, 1988.
(9) Lehn, J.-M. *Supramolecular Chemistry: Concepts and Perspectives*; VCH: Weinheim, 1995.
(10) Binder, W. H., *Hydrogen Bonded Polymers*; Springer: Berlin, 2007.
(11) Hamley, I. W. *Angew. Chem., Int. Ed.* **2007**, *46*, 8128–8147.
(12) König, H. M.; Kilbinger, A. F. M. *Angew. Chem., Int. Ed.* **2007**, *46*, 8334–8340.
(13) Gress, A.; Smarsly, B.; Schlaad, H. *Macromol. Rapid Commun.* **2008**, *29*, 304–308.
(14) Thijs, H. M. L.; Becer, C. R.; Guerro-Sanchez, C.; Fournier, D.; Hoogenboom, R.; Schubert, U. S. *J. Mater. Chem.* **2007**, *17* 4864–4871.
(15) Liang, Y.-Z.; Li, Z.-C.; Li, F.-M. *J. Colloid Interface Sci.* **2000**, *224*, 84–90.
(16) Gress, A.; Völkel, A.; Schlaad, H. *Macromolecules* **2007**, *40* 7928–7933.
(17) Förster, S.; Burger, C. *Macromolecules* **1998**, *31*, 879–891.
(18) Schlaad, H.; You, L.; Sigel, R.; Smarsly, B.; Heydenreich, M.; Mantion, A.; Mašić, A. *Chem. Commun.* **2009**, 1478–1480.
(19) Dai, J.; Goh, S. H.; Lee, S. Y.; Slow, K. S. *J. Appl. Polym. Sci.* **1994**, *53*, 837–845.
(20) Friebolin, H. *Basic One- and Two-Dimensional NMR-Spectroscopy*; VCH Verlagsgesellschaft: Weinheim, 1991.
(21) *Polymer Handbook*, 3rd ed.; Brandrup, J., Immergut, E. H., Eds.; Wiley-Interscience: New York, 1989.